Materials Science & Engineering C 108 (2020) 110391

Contents lists available at ScienceDirect

Materials Science & Engineering C

journal homepage: www.elsevier.com/locate/msec

Selective patterning of netrin-1 as a novel guiding cue for anisotropic dendrogenesis in osteocytes

Aira Matsugaki, Daisuke Yamazaki, Takayoshi Nakano*

Division of Materials and Manufacturing Science, Graduate School of Engineering, Osaka University, 2-1, Yamadaoka, Suita, Osaka, 565-0871, Japan

ARTICLE INFO

Keywords:
Extracellular matrix
Netrin-1
Osteocyte
Dendrite
Anisotropic dendrogenesis
Inkjet printing

ABSTRACT

Although protein patterning approaches have found widespread applications in tuning surface characteristics of biomaterials, selective control of growth in cell body and dendrites utilizing such platforms remains difficult. The functional roles assumed by cell body and dendrites in a physiological milieu have extremely high specificity. In particular, osteocytes embedded inside the mineralized bone matrix are interconnected via dendritic cell processes characterized by an anisotropic arrangement of the lacunar-canalicular system, where the fluid-flow inside the canaliculi system regulates the mechanoresponsive functionalization of bone. Control of cellular networks connected by dendritic cell processes is, therefore, imperative for constructing artificially controlled bone-mimetic structures and as an extension, for gaining insights into the molecular mechanisms underlying dendrogenesis inside the mineralized bone matrix. Here, we report an innovative strategy to induce controlled elongation of cell body or dendritic process structures in selective directions by using the inkjet printing technique. Artificial runways employing netrin-1, inspired by neural architecture, were utilized to trigger controlled elongation in the osteocyte dendritic processes in desired directions. This is the first report, to the best of our knowledge, demonstrating that anisotropic dendrogenesis of osteocytes can be controlled with selective patterning of extracellular proteins, specifically via the axon guidance ligand netrin-1.

1. Introduction

The morphological characteristics of living systems, imperative for the realization of organ or tissue-specific functions, is exerted by spatiotemporal regulation of the functional roles assumed by various proteins. In particular, the mechanical function of bone tissue is mainly governed by the highly ordered arrangement of collagen matrix/apatite crystals [1,2]. Osteoblasts, in conjunction with the osteocyte network, are involved in the process of bone formation [3]. Importantly, the cellular arrangement in osteoblasts has been linked to the ordered architecture and orientation of the mineralized bone matrix [4–7]. Osteocytes, the most abundant cell type in bones, are derived from bone-forming osteoblasts that become embedded in the extracellular matrix they secrete. Osteocytes are now recognized as crucial orchestrators of skeletal homeostasis, which control both osteoblastic bone formation and osteoclastic bone resorption by transducing mechanical stimuli into biochemical signals [8]. In intact bone tissue, osteocytes are arranged in an ordered manner inside the mineralized matrix with their cell bodies parallel to the lamellar bone, with the dendritic cellular processes running perpendicular to the cell bodies [9,10]. The anisotropic lacunar-canaliculi network facilitates the osteocyte-mediated mechanosensation and transduction [11]. In fact, bone diseases and disorders are associated with an orchestrated disarrangement in the orientation of both bone matrix and anisotropic osteocyte network [12]. Therefore, gaining control over the bone-mimetic osteocyte network as well as anisotropic bone microstructure is imperative for the realization of functional recovery of the bone tissue.

At the developmental stage, spatiotemporally distinct expression of biological signals triggers tissue or organ-specific pattern formation [13]. Among them, dendrite morphogenesis in the nervous system has been well studied and its strict control by multiple regulatory pathways demonstrated [14]. However, osteocyte dendrogenesis in bone tissue is poorly understood. Extracellular cues governing dendrite morphogenesis probably regulate the osteocyte network structure in ways similar to that observed in the nervous system. In this study, controlled elongation of osteocyte cell bodies and dendrites in specific directions was

Abbreviations: Cx43, Connexin 43; DCC, Deleted in Colorectal Cancer; DDW, Distilled Deionized Water; EDTA, ethylenediaminetetraacetic acid; FAK, Focal Adhesion Kinases; FBS, Fetal Bovine Serum; HBSS, Hank's Balanced Salt Solution; α-MEM, Minimum Essential Medium Eagle - alpha modification; NDS, Normal Donkey Serum; NGS, Normal Goat Serum; PBST, Phosphate Buffered Saline-0.05% Triton X-100

* Corresponding author.
E-mail address: nakano@mat.eng.osaka-u.ac.jp (T. Nakano).

https://doi.org/10.1016/j.msec.2019.110391
Received 25 July 2019; Received in revised form 2 October 2019; Accepted 31 October 2019
Available online 05 November 2019

achieved by using the inkjet printing technology, which affords geometrically controlled material deposition and patterning [15]. We specifically focused on probing the role of extracellular matrix cues related to axon morphogenesis in neurons. In nervous system, the cellular processes involving dendrites and axons, which show characteristic structures similar to the dendrites in osteocyte, are strictly regulated by specific guidance cues. Among multiple types of axon guidance factors, netrin-1 has been recognized as a crucial regulator in axon outgrowth during central nervous system development and shown to be involved in the morphogenesis of organs [16,17]. The above evidence of netrin-1 as a powerful regulator in axon guidance in nervous system led us to hypothesize the involvement of netrin-1 in the formation of osteocyte dendritic processes in bone tissue. To the best of our knowledge, we report for the first time that axonal guidance cues work as extrinsic factors for osteocyte dendrogenesis.

2. Materials and methods

2.1. Fabrication of micropatterned substrates coated with cell adhesion molecules

The micropatterned substrates coated with specific proteins were fabricated by the inkjet printing procedure (Fig. 1). Prior to printing, all the cover glasses (ϕ13 mm, Matsunami, Osaka, Japan) were sterilized with 70% ethanol and DDW. First, to reduce non-specific surface attachment of cells, the cover glasses were coated with 0.1% 2-methacryloyloxyethyl phosphorylcholine (Lipidure, Nichiyu, Japan) and dried at 50 °C for an hour. Then, the desired patterns were drawn with a Pulse Injector (Cluster Technology, Osaka, Japan) as follows. Cross patterning was achieved by the combination of line patterning with 0.2 mg/ml fibronectin (R&D systems, Minneapolis, MO) and dot patterning with 1 μg/ml netrin-1 (R&D systems, Minneapolis, MO), followed by incubation at 37 °C for 12 h. The ejection procedure was controlled using a WaveBuilder (Cluster Technology, Osaka, Japan) with regulatory parameters of wave profile, voltage, and ejection number per second. The voltage impulse to eject a droplet was set at 8.6 V for line patterning and 4.6 V for dot pattering. Droplet ejection frequency was set to 750 Hz. The obtained micropatterned substrates were washed five times with DDW, followed by sterilization with UV irradiation.

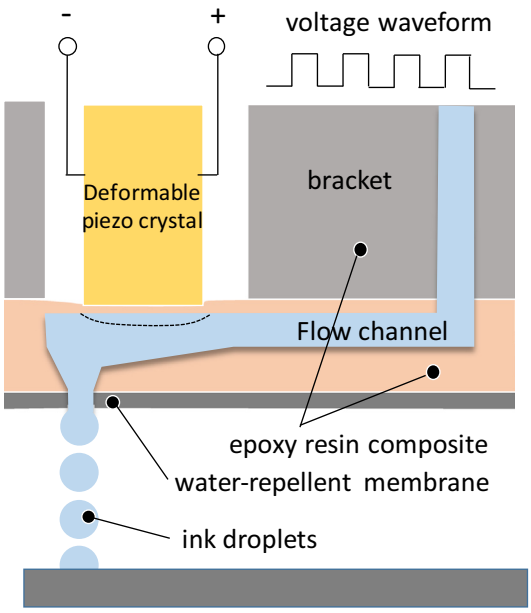

Fig. 1. Schematic illustration of piezoelectric injectors with 25 μm-sized nozzles. Printing of proteins can be controlled by regulating the ejection parameters involving voltage impulse and droplet numbers.

2.2. Osteocyte isolation and culture

Primary osteocytes were isolated from murine long bones (femurs, tibiae, and humeri) with a sequential digestion protocol [18]. Briefly, femurs, tibiae, and humeri from skeletally mature C57BL/6 J mice were placed in fresh α-MEM (Invitrogen, Carlsbad, CA) with penicillin and streptomycin, and fibrous tissues around the bone were removed. These bones were then cut into segments of 1–2 mm length and washed with HBSS. The segments were subjected to nine cycles of digestion at 37 °C for 25 min each. In the first three digestions, bone chips were incubated with 2 mg/mL collagenase type I (Wako, Osaka, Japan) dissolved in α-MEM and washed thrice in HBSS. From the fourth digestion, bone chips were incubated with EDTA (Nacalai Tesque, Kyoto, Japan) and collagenase in turns and washed thrice in HBSS each. Subsequently, the digested bone chips were cut again and plated in dishes with α-MEM supplemented with 10% fetal bovine serum (FBS) and 200U/mL penicillin and streptomycin. Osteocytes migrated from the bone chips after 7–10 days cultivation were detached by incubation with 0.25% trypsin/EDTA solution, followed by the seeding to the patterned substrates. Temporal evolution of dendrogenesis was visualized using gridded glass-bottom dishes (MatTek, Ashland, MA) with phase-contrast microscopy in a Biozero setup (Keyence Corporation, Osaka, Japan).

2.3. Gene expression

Total RNA was extracted using TRIzol reagent (Invitrogen, Paisley, UK). The levels of SOST mRNA relative to GAPDH in isolated osteoblasts and osteocytes were analyzed by using quantitative real-time PCR in accordance with the manufacture's guidelines (Step-one, Applied Biosystems). The threshold number of cycles (Ct) was set within the exponential phase of the PCR reaction, and the ΔCt value for the target gene was calculated by subtracting the Ct value of GAPDH (internal control) from the target gene. Results are displayed as the relative expression (percentage) compared to GAPDH expression, and normalized relative to the osteoblasts-enriched digestion.

2.4. Fluorescence imaging

For visualization of substrate patterning, the micropatterned substrates were first washed twice with PBS. Then, the substrates were incubated with 1% normal goat serum (NGS; Invitrogen, Carlsbad, CA) for 30 min at room temperature to block non-specific reactions. Then the substrates were treated with primary antibodies (chicken antibodies against netrin-1 (Abcam, Cambridge, UK) and rabbit antibodies against fibronectin (Abcam, Cambridge, UK)) for 12 h at 4 °C. After washing with PBS-0.05% Triton X-100 (PBST), substrates were incubated with the secondary antibodies (Alexa Fluor 594 goat anti chicken IgY (Molecular Probes/Invitrogen, Eugene, OR), and Alexa Fluor 488 goat anti rabbit IgG (Molecular Probes/Invitrogen, Eugene, OR)) for 90 min at room temperature. After washing with PBST, the substrates were mounted in Prolong Gold antifade reagent (Molecular Probes/Invitrogen, Eugene, OR).

For immunocytochemistry of DCC (deleted in colorectal cancer) in osteocytes, the cells were fixed with 4% paraformaldehyde. Next, the cells were kept in PBST containing 5% normal donkey serum (NDS; Invitrogen, Carlsbad, CA) for 30 min at room temperature to block non-specific reactions. The cells were then incubated with the primary antibody (goat against DCC (Santa Cruz Biotechnology Inc., Dallax, TX)) for 12 h at 4 °C. After washing with PBST, cells were labeled with the secondary antibody (Alexa Fluor 594 donkey anti goat IgG (Molecular Probes/Invitrogen, Eugene, OR)) for 90 min at room temperature, followed by washing with PBST. Subsequently, the cells were incubated with Alexa Fluor 488 phalloidin (Molecular Probes/Invitrogen, Eugene, OR). Then, the cells were washed with PBST and mounted in Prolong

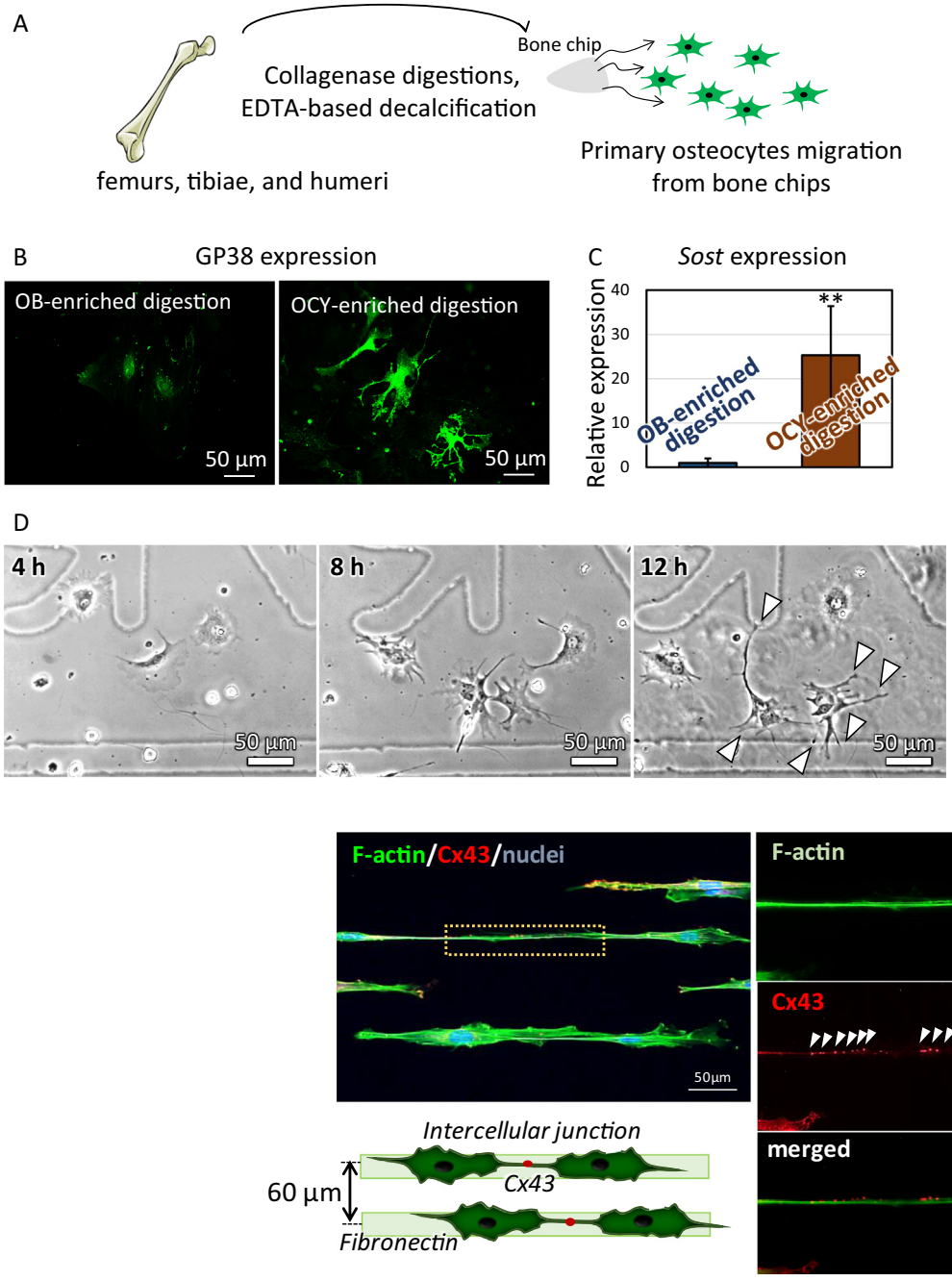

Fig. 2. (A) Schematic illustration of the isolation of primary osteocytes from mature long bones. (B) Immunocytochemical analysis of GP38 expression in the isolated cellular digestions. (C) Quantitative analysis of *Sost* expression in the isolated cells depending on the digestion process. (D) (B) Phase-contrast images of dendrogenesis in isolated osteocyte-like cells after 4 h, 8 h, and 12 h of cell seeding. Arrowheads indicate the elongation of dendrites from cell bodies. **; $p < 0.01$.

Fig. 3. Control of osteocyte adhesion by line-patterned fibronectin coating. Cx43-positive gap junctions are expressed between neighboring osteocyte-like cells. Each cell shows an elongated morphology with poor generation of dendrites.

Gold antifade reagent with DAPI. Images were obtained using a fluorescence microscope (Biozero, Keyence Corporation, Osaka, Japan). The immunocytochemical analysis of the expression of osteocytic marker GP38 was carried out in the above-mentioned same conditions with blocking in 5% normal goat serum (NGS; Invitrogen, Carlsbad, CA) followed by the incubation with the primary antibody (hamster against GP38 (Santa Cruz Biotechnology Inc., Dallax, TX) and the secondary antibody (Alexa Fluor 488 goat anti hamster IgG (Molecular Probes/Invitrogen, Eugene, OR)).

2.5. Quantitative analysis of dendritic processes

The extension direction of the dendritic processes was quantitatively analyzed by using ImageJ (NIH) after cultivation for 24 h. The quantitative analysis of dendrite length and angle was performed in the 35 images of 443 μm × 333 μm area per group. The angle between dendritic process and fibronectin line patterning (θ) was measured. Only dendritic processes with length of more than 20 μm was counted. To quantitatively evaluate the degree of alignment of dendritic processes, the vertical component of fibronectin patterning was taken as a reference. The dendritic processes were found to be elongated by a range of ± 40° with respect to the reference. The degree of dendrite orientation was characterized by the angular standard deviation, S.D. (σ) with the following equations:

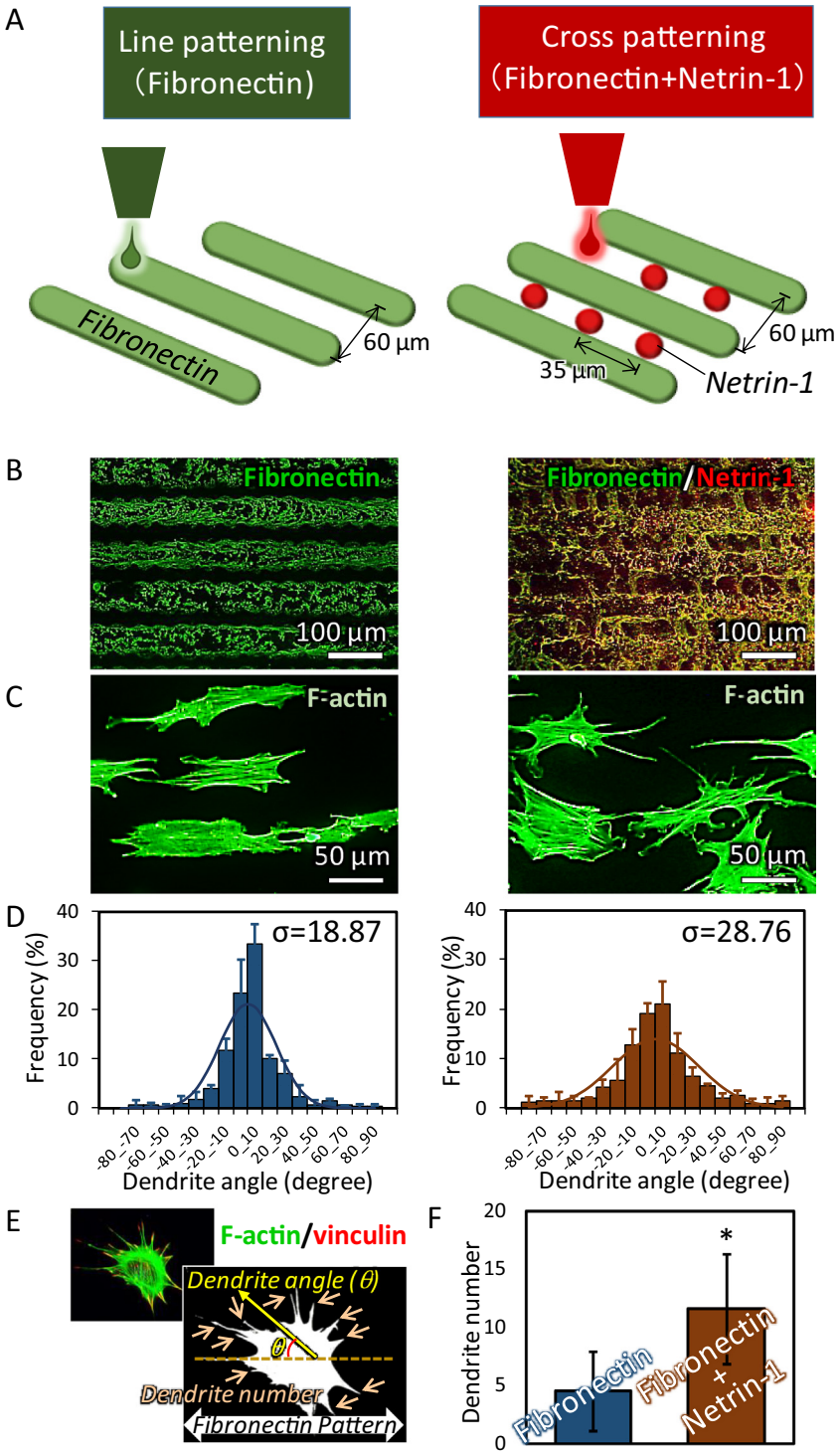

Fig. 4. Control of osteocyte dendrogenesis by combined patterning of fibronectin and netrin-1. (A) Schematic illustration of protein patterning approach. (B) Immunofluorescence images of patterned proteins. Green; fibronectin. Red; netrin-1. (C) Immunofluorescence images of osteocytes adhered on the prepared substrates with specific patterns. (D) Distribution histogram of elongation angles of dendrites from cell body. The inset value of σ shows the angular standard deviation calculated from the dendrite angles. (E) The orientation and number of dendrites were analyzed based on the fluorescence images. (F) The number of cellular dendrites per single cell. *; $p < 0.05$. (For interpretation of the references to color in this figure legend, the reader is referred to the Web version of this article.)

$$\rho = \frac{1}{n}\sqrt{\left(\sum_{i=1}^{n} \cos 2\theta_i\right)^2 + \left(\sum_{i=1}^{n} \sin 2\theta_i\right)^2},$$

$$\sigma = \frac{1}{2}\sqrt{-2\ln\rho}$$

where, n is the number of dendrites.

2.6. Statistical analysis

Statistical significance was tested using the Student's *t*-test or Welch's *t*-test between two groups. If there are three or more groups, Tukey's multiple test was applied. A significance of $p < 0.05$ was required for rejecting the null hypothesis.

3. Results

3.1. Osteocyte dendrogenesis

The isolated cells demonstrated dendrite-rich morphology typical to osteocytes after a minimum of 8 h of culture, followed by maturation and elongation of dendrites after 12 h of culture (Fig. 2). The isolated osteocytes phenotypes were also confirmed by quantitative gene

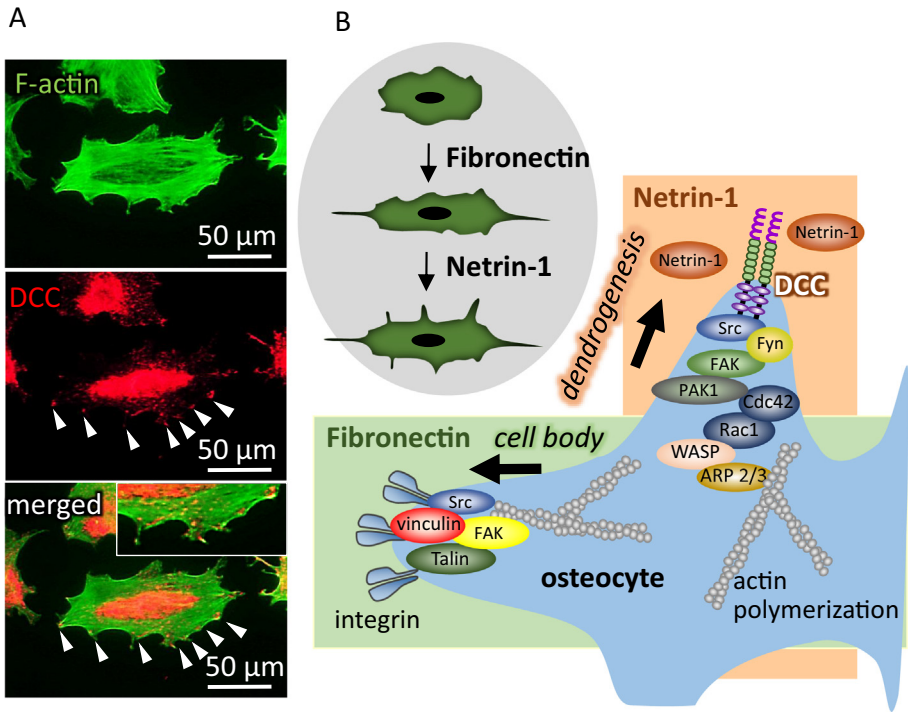

Fig. 5. (A) Immunofluorescence images of DCC expression in osteocytes adhered on substrates patterned with fibronectin and netrin-1. Arrowheads indicate the positive expression of DCC at the dendrogenesis region in osteocyte. Green; F-actin, Red; DCC. (B) Schematic diagram of control of osteocyte dendrogenesis via combined patterning of fibronectin and netrin-1. (For interpretation of the references to color in this figure legend, the reader is referred to the Web version of this article.)

expression analysis and immunocytochemical analysis of osteoblastic digestion (digestion 7) and osteocytic digestion (digestion 9). The initial stage of osteocytic marker GP38 was strongly expressed in the isolated osteocyte-enriched digestion, whereas it was not detected in the osteoblast digestion. Gene expression analysis using realtime RT-PCR revealed that the positive expression of *Sost* gene encoding sclerostin in osteocyte-enriched digestion (bone fragment) compared to osteoblast-enriched digestion (digestion 5). Line patterning with fibronectin allowed the cells to adhere along the patterned lines via connexin 43 (Cx43)-positive intercellular junctions (Fig. 3).

3.2. Ordered cell body adhesion on fibronectin patterning and dendritic formation along netrin-1 patterning

Fluorescence microscopy images revealed that combined anisotropic patterning of fibronectin and netrin-1 was successfully obtained by the inkjet printing procedure (Fig. 4). The specific line patterning with fibronectin was controlled less than the width of 50 μm for adhesion of osteocyte cell bodies, and dot patterning with netrin-1 was controlled less than 20 μm for osteocytes to extend their dendritic processes.

Fabricated micropatterned substrates allowed specific adhesion of osteocyte cell bodies on fibronectin patterning both in case of line patterning and cross patterning. Osteocytes elongated both cell bodies and dendritic processes along the fibronectin patterning (Fig. 4B). The histograms in Fig. 4D show the distribution of dendritic process orientation on each substrate. The quantitative analysis of directional distribution of dendritic processes revealed that netrin-1 has significant effects on dendritic process extension and attraction. In addition, DCC was highly expressed at the sites of dendrogenesis (Fig. 5).

4. Discussion

We developed an innovative method to induce targeted and selective elongation of osteocyte dendritic processes by culturing primary osteocytes on specially designed micropatterned substrates containing a cross pattern of fibronectin and netrin-1. To the best of our knowledge, our results constitute the first report on the crucial regulatory role of netrin-1 in osteocyte dendritic process formation. Cell patterning is a powerful strategy for biomimetic organ or tissue construction. Bone-mimetic microstructures have been engineered using electrophoresis-based cell patterning [19] and microcontact printing techniques [20]. Although previous reports have demonstrated the manipulation of various cell types with bone-mimetic patterning, selective modulation of osteocyte dendrogenesis, a key regulator of bone mechanosensation, has never been explored. In this study, we report, for the first time, the role of netrin-1 as a dendrogenesis regulator in bone. Netrins were first identified as guidance cues, directing axon migration during neural development [16]. Recently, netrins have been found to play key roles in several tissues outside the nervous system involving pancreas, lung, and the vascular system [17]. In bone tissue, netrin-1 is secreted by osteoclasts and functions in autocrine/paracrine manner for osteoclast differentiation [21]. Netrin-1 expression is also induced in osteoblasts and synovial fibroblasts stimulated with IL-17 [22], whereas the expression of netrin-1 in osteocytes is still unclear. Although emerging evidence indicates that netrin-1 is an essential regulatory molecule for bone metabolism, the role of netrin-1 in osteocytes is largely unknown. Netrin-1 acts as a chemoattractant in axon growth cones through the receptor DCC [23]. Netrin-1/DCC signaling guides neuronal migration by mediating the activation of constitutively bound NCK1 and focal adhesion kinases (FAK), followed by the recruitment of a number of intracellular signaling components that activate Src family kinases and Rho GTPases, and ultimately the rearrangement of the actin cytoskeleton [24]. In this study, the dendritic cell processes were observed to elongate selectively on micropatterned netrin-1. In addition, DCC was found to be expressed at the localized dendrogenesis positions in osteocytes. DCC was also detected inside the cell bodies as is reported in the previous works [25,26], in spite that the dendrite extension is mainly regulated by DCC1 expression localized at the initiating positions of dendrites. These results indicate that osteocytes elongate their dendritic processes in response to netrin-1 molecules via DCC-mediated signaling, following which the actin cytoskeleton rearranges to direct the processes along the cytoskeletal meshwork. There is now increasing evidence that nervous system and bone metabolism express some common signaling molecules [27]. The other types of axon guiding cues other than netrin-1 also possibly control the osteocyte dendrogenesis

and they will be reported in future.

The successful control of anisotropic osteocyte network demonstrated in our work is envisioned to a promising tool for the development of artificially regulated cellular components for medical applications. In addition, our results aid in gaining insights into the molecular scenario facilitating the multicellular organization associated with bone tissue construction, especially in identifying the contributor for its anisotropic microstructure. In spite that the complex contacts between the cells and bone matrix is necessary for the mechanosensing functions in osteocytes, the significance of the present model which represents a simplified two-dimensional culture platform is to find out the candidate molecule for osteocyte dendrogenesis and further development for control of osteocyte functions. The present culture model represents osotecyte networks inside the lacunar-canaliculi system, which enable to visualize and find out the molecular mechanisms for bone tissue development. Although the precise mechanism regulating netrin-1 induced attraction of dendritic processes in osteocyte is still not fully understood, netrin-1/DCC signaling is one of the contributing pathways for osteocyte cytoskeletal dynamics (Fig. 5).

5. Conclusion

Cellular networks play important roles in tissue-specific function. In this study, we have demonstrated an innovative method to control anisotropic osteocyte network by selective positioning of cell body or dendritic process structures at precise locations. The guiding cue, composed of combined patterns of fibronectin and netrin-1, was effective in triggering selective adhesion of cell body and elongation of dendrites. Our results constitute novel evidence on the role of axon guidance factor netrin-1 in controlling dendritic processes in osteocytes and offer crucial insights into the molecular mechanisms regulating oriented microstructure formation in bone tissue.

Declaration of competing interest

The authors declare no conflict of interest. The funders had no role in the design of the present study; in the collection, analyses, or interpretation of data; in the writing of the manuscript, and in the decision to publish these results.

Acknowledgements

This research was funded by Grants-in-Aid for Scientific Research (S) (grant number 18H05254), and Challenging Research (Pioneering) (grant number 17H06224).

References

[1] T. Nakano, K. Kaibara, T. Ishimoto, Y. Tabata, Y. Umakoshi, Biological apatite (BAp) crystallographic orientation and texture as a new index for assessing the microstructure and function of bone regenerated by tissue engineering, Bone 51 (2012) 741–747, https://doi.org/10.1016/j.bone.2012.07.003.

[2] T. Ishimoto, T. Nakano, Y. Umakoshi, M. Yamamoto, Y. Tabata, Degree of biological apatite c-axis orientation rather than bone mineral density controls mechanical function in bone regenerated using recombinant bone morphogenetic protein-2, J. Bone Miner. Res. 28 (2013) 1170–1179, https://doi.org/10.1002/jbmr.1825.

[3] A. Gupta, H. Anderson, A.M. Buo, M.C. Moorer, M. Ren, J.P. Stains, Communication of cAMP by connexin43 gap junctions regulates osteoblast signaling and gene expression, Cell. Signal. 28 (2016) 1048–1057, https://doi.org/10.1016/j.cellsig.2016.04.014.

[4] A. Matsugaki, N. Fujiwara, T. Nakano, Continuous cyclic stretch induces osteoblast alignment and formation of anisotropic collagen fiber matrix, Acta Biomater. 9 (2013) 7227–7235, https://doi.org/10.1016/j.actbio.2013.03.015.

[5] A. Matsugaki, G. Aramoto, T. Ninomiya, H. Sawada, S. Hata, T. Nakano, Abnormal arrangement of a collagen/apatite extracellular matrix orthogonal to osteoblast alignment is constructed by a nanoscale periodic surface structure, Biomaterials 37 (2015) 134–143, https://doi.org/10.1016/j.biomaterials.2014.10.025.

[6] R. Ozasa, A. Matsugaki, Y. Isobe, T. Saku, H.S. Yun, T. Nakano, Construction of human induced pluripotent stem cell-derived oriented bone matrix microstructure by using in vitro engineered anisotropic culture model, J. Biomed. Mater. Res. A 106 (2018) 360–369, https://doi.org/10.1002/jbm.a.36238.

[7] A. Matsugaki, Y. Isobe, T. Saku, T. Nakano, Quantitative regulation of bone-mimetic, oriented collagen/apatite matrix structure depends on the degree of osteoblast alignment on oriented collagen substrates, J. Biomed. Mater. Res. A 103 (2015) 489–499, https://doi.org/10.1002/jbm.a.35189.

[8] M.B. Schaffler, W.Y. Cheung, R. Majeska, O. Kennedy, Osteocytes: master orchestrators of bone, Calcif. Tissue Int. 94 (2014) 5–24, https://doi.org/10.1007/s00223-013-9790-y.

[9] Y. Sugawara, H. Kamioka, Y. Ishihara, N. Fujisawa, N. Kawanabe, T. Yamashiro, The early mouse 3D osteocyte network in the presence and absence of mechanical loading, Bone 52 (2013) 189–196, https://doi.org/10.1016/j.bone.2012.09.033.

[10] L.F. Bonewald, Generation and function of osteocyte dendritic processes, J. Musculoskelet. Neuronal Interact. 5 (2005) 321–324.

[11] T. Nakano, T. Ishimoto, N. Ikeo, A. Matsugaki, Advanced analysis and control of bone microstructure based on a materials scientific study including microbeam X-ray diffraction, in: T. Kakeshita (Ed.), Progress in Advanced Structural and Functional Materials Design, Springer, Japan, 2013, pp. 155–167.

[12] A. Sekita, A. Matsugaki, T. Ishimoto, T. Nakano, Synchronous disruption of anisotropic arrangement of the osteocyte network and collagen/apatite in melanoma bone metastasis, J. Struct. Biol. 197 (2017) 260–270, https://doi.org/10.1016/j.jsb.2016.12.003.

[13] A. Sivakumar, N.A. Kurpios, Transcriptional regulation of cell shape during organ morphogenesis, J. Cell Biol. 217 (2018) 2987–3005, https://doi.org/10.1083/jcb.201612115.

[14] F.J. Bustos, N. Jury, P. Martinez, E. Ampuero, M. Campos, S. Abarzúa, K. Jaramillo, S. Ibing, M.D. Mardones, H. Haensgen, J. Kzhyshkowska, M.F. Tevy, R. Neve, M. Sanhueza, L. Varela-Nallar, M. Montecino, B. van Zundert, NMDA receptor subunit composition controls dendritogenesis of hippocampal neurons through CAMKII, CREB-P, and H3K27ac, J. Cell. Physiol. 232 (2017) 3677–3692, https://doi.org/10.1002/jcp.25843.

[15] B. Derby, Bioprinting: inkjet printing proteins and hybrid cell-containing materials and structures, J. Mater. Chem. 18 (2008) 5717–5721, https://doi.org/10.1039/B807560C.

[16] K.L.W. Sun, J.P. Correia, T.E. Kennedy, Netrins: versatile extracellular cues with diverse functions, Development 138 (2011) 2153–2169, https://doi.org/10.1242/dev.044529.

[17] J.B. Bongo, D.Q. Peng, The neuroimmune guidance cue netrin-1: a new therapeutic target in cardiovascular disease, J. Cardiol. 63 (2014) 95–98, https://doi.org/10.1016/j.jjcc.2013.10.006.

[18] A.R. Stern, M.M. Stern, M.E. Van Dyke, K. Jähn, M. Prideaux, L.F. Bonewald, Isolation and culture of primary osteocytes from the long bones of skeletally mature and aged mice, Biotechniques 52 (2012) 361–373, https://doi.org/10.2144/0000113876.

[19] C.-T. Ho, R.-Z. Lin, W.-Y. Chang, H.-Y. Chang, C.-H. Liu, Rapid heterogeneous liver-cell on-chip patterning via the enhanced field-induced dielectrophoresis trap, Lab Chip 6 (2006) 724–734, https://doi.org/10.1039/B602036D.

[20] X.L. Lu, B. Huo, M. Park, X.E. Guo, Calcium response in osteocytic networks under steady and oscillatory fluid flow, Bone 51 (2012) 466–473, https://doi.org/10.1016/j.bone.2012.05.021.

[21] A. Mediero, B. Ramkhelawon, M. Perez-Aso, K.J. Moore, B.N. Cronstein, Netrin-1 is a critical autocrine/paracrine factor for osteoclast differentiation, J. Bone Miner. Res. 30 (2015) 837–854, https://doi.org/10.1002/jbmr.2421.

[22] K. Maruyama, T. Kawasaki, M. Hamaguchi, M. Hashimoto, M. Furu, H. Ito, T. Fujii, N. Takemura, T. Karuppuchamy, T. Kondo, T. Kawasaki, M. Fukasaka, T. Misawa, T. Saitoh, Y. Suzuki, M.M. Martino, Y. Kumagai, S. Akira, Bone-protective functions of netrin 1 protein, J. Biol. Chem. 291 (2016) 23854–23868, https://doi.org/10.1074/jbc.M116.738518.

[23] C. Laumonnerie, R.V. Da Silva, A. Kania, S.I. Wilson, Netrin 1 and Dcc signalling are required for confinement of central axons within the central nervous system, Development 141 (2014) 594–603, https://doi.org/10.1242/dev.099606.

[24] G. Liu, H. Beggs, C. Jürgensen, H.-T. Park, H. Tang, J. Gorski, K.R. Jones, L.F. Reichardt, J. Wu, Y. Rao, Netrin requires focal adhesion kinase and Src family kinases for axon outgrowth and attraction, Nat. Neurosci. 7 (2004) 1222–1232, https://doi.org/10.1038/nn1331.

[25] M. Shekarabi, T.E. Kennedy, The netrin-1 receptor DCC promotes filopodia formation and cell spreading by activating Cdc42 and Rac1, Mol. Cell. Neurosci. 19 (2002) 1–17, https://doi.org/10.1006/mcne.2001.1075.

[26] M. Meriane, J. Tcherkezian, C.A. Webber, E.I. Danek, I. Triki, S. McFarlane, E. Bloch-Gallego, N. Lamarche-Vane, Phosphorylation of DCC by Fyn mediates Netrin-1 signaling in growth cone guidance, J. Cell Biol. 167 (2004) 687–698, https://doi.org/10.1083/jcb.200405053.

[27] P. Dimitri, C. Rosen, The central nervous system and bone metabolism: an evolving story, Calcif. Tissue Int. 100 (2017) 476–485, https://doi.org/10.1007/s00223-016-0179-6.